

SLIDING OF WATERPROOFING LAYERS

C. DE BACKER and L. FRANCKEN

Centre de Recherches Routieres
Brussels, Belgium

When waterproofing is placed on an inclined base, shear stresses take place parallel to the slope as a result of the dead load of the layers placed on top of the waterproofing layer and sticking to it.

Sliding of the whole system can result from either creep of the waterproofing layer or lack of friction at the base-waterproofing interface when the latter is not adhered to the base. This phenomenon can cause longitudinal joints to open or create very wide cracks oriented perpendicularly to the direction of the slope (*Figure 1*).

In the case of bridge decks, the main concern of the research program carried out at the Belgian Road Research Centre, these defects can be responsible for corrosion of the structure and its steel reinforcement. Due to the high cost of maintaining and rehabilitating these structures, and the difficulties associated with repair, it was considered worthwhile to set up a rational method for designing waterproofing by taking into account the physical characteristics of the components of the road structure.

The present paper presents some of the main results of this research project.

PREDICTING THE CREEP SLIDING MECHANISM

The assessment of the displacement caused by sliding of a waterproofing layer over a period of several years is a major criterion in the sound choice of a technical solution. The structures considered in the present study consist of different materials superimposed to form stratified systems similar to the three layer structure schematically represented in *Figure 2*.

In assessing the behavior of the waterproofing, only this latter was considered to be subject to deformation.

The elementary displacement, dI , of the upper undeformed part of the structure during the time interval, dt , at the temperature, T , is given by:

$$dI = \frac{\tau h_3 dt}{\eta(t, T)}$$

in which $\eta(t, T)$ is the coefficient of viscosity of the deformable material after t seconds and at temperature T , τ is the magnitude of the shearing stress acting onto the deformable waterproofing underlayer, and h_3 is the thickness of the waterproofing layer (*Figure 2*).

The total displacement, L , after loading time, t_1 , may then be obtained by integration:

$$L = \tau h_3 \int_0^{t_1} \frac{dt}{\eta(t, T)} \quad (1)$$

This is the basic formula used to calculate the magnitude of sliding.

The data needed are:

- the value of the shearing stress τ ,
- the coefficient of viscosity η of the deformable material,
- the temperature T in the structure over a period of one year.

The evaluation of these data for practical application will be explained in the next three sections.

Evaluation of the shearing stress

The analysis presented hereafter does not take into account the effect of static or moving loads which could act on the top layer. Hence, the deformable layer is supposed to be submitted only to the dead load of the upper layers.

When the supporting surface is inclined at an angle, α , as shown in *Figure 2*, the shearing stress acting on the underlayer has a mean value given by:

$$\tau = (h_1 \cdot \rho_1 + h_2 \cdot \rho_2 + 0,5 \cdot h_3 \cdot \rho_3) \cdot g \cdot \sin \alpha \quad (2)$$

where h_1 , h_2 , h_3 are the thicknesses of the different layers, and ρ_1 , ρ_2 , ρ_3 are the volumic masses of the different layers.

This formula can of course be generalized to a greater number of layers. Nevertheless this simple model is quite satisfactory for the purpose of comparing different waterproofing systems.

Experimental Viscosity Determination

The materials or combinations of materials making up part of the deformable layer must be tested under stress and environmental conditions as close as possible to actual service conditions.

■ Experimental Layout

To do this, a very simple procedure is used in which a sample of the material maintained at a constant temperature is submitted to a constant shearing stress. The information is obtained by recording the resulting deformation of the sample as a function of time.

The sample has the shape of a parallelepiped. It is fixed between two parallel rectangular metallic plates with an epoxy resin in order to form a sandwich of thickness D . One of the metallic plates is secured to the apparatus, while the other is loaded by a weight acting in the plate-material interface plane. An LVDT displacement transducer attached to the movable plate permits measurement and continuous recording of the long-term deformations of the sample. A microprocessor controls starting the procedure, temperature, data acquisition and final processing including graphical plotting and numerical print-out of results.

Based on the type of waterproofing, two different versions of the experimental device were utilized.

1. For bituminous binders, mastic, poured asphalt or mortars, in which the grain size does not exceed 2mm, the specimens were 3cm long, 2cm wide and 1cm thick.

The experimental device, which is shown in Figure 3, is the sliding plate rheometer developed by Fenyn and Krooshof.¹ The applied stresses are in the range of 650 to 4700 Pascal. The temperatures may be maintained constant in the range from -10 to +60C.

2. For the study of the behavior of waterproofings imbedded in a full structure, including the supporting concrete, the waterproofing layer and the upper layers, a larger device was specially developed (Figure 4). The specimens are 20cm long, 4cm wide and 4cm thick. The device was designed for testing four specimens at the same time at the same temperature.

It has been verified that the results provided by both devices are in agreement, taking experimental error into account.

In the case of waterproofing systems, consisting of a superposition of prefabricated sheets, the test gives information on the mean overall behavior of the waterproofing and on the adhesive used to glue it to the base material. A close observation of the deformed sample after testing may be very important in order to determine the contribution of the different interlayers to the total deformation.

Figure 5 shows a waterproofing sheet glued with bitumen to the base cement concrete. It is clear that the main contribution to deformation comes from the bitumen.

■ Interpretation of results

The deformation of the specimen as a function of time is immediately observable in the form of a creep curve showing the evolution of the angular shear $\gamma = d1/h_1$.

The data acquisition system takes nearly one hundred readings of displacement and time during each test.

From these data the interpretation program deduces about 20 values of the shear rate, $\dot{\gamma}$, by deriving the angular shear with respect to time. Then the value of the coefficient of viscosity for the corresponding time interval is obtained by:

$$\eta(t, T) = \frac{t}{\dot{\gamma}}$$

This interpretation method allows us to obtain the isotherms of the viscosity curves in terms of time.

In the range of low stresses and long times, the material exhibits a nonlinear creep curve. As a result, the coefficient of viscosity is an increasing function of time.

Notice also that the use of the viscosity concept rather than stiffness eliminates the lack of reliability and reproducibility existing at the very first moments of loading. This effect is unavoidable in such a test and is responsible for uncontrollable shifts of the whole stiffness curve.

■ Master Viscosity Curve

In all cases studied so far, including waterproofings made up of different layers, viscosity displays a dependence on time which is linear in a bilogarithmic scale (Figure 6). These observations were made at temperatures ranging from -12C to 60C and over a time range of up to 30,000 seconds. For a fixed temperature, T, the viscosity is given by a function of the form:

$$\eta(t, T) = K(T) \cdot t^b \quad (3)$$

where K(T) is a function of temperature and b is a parameter.

Moreover it has been verified that the principle of

temperature and time interchangeability is valid for most of the materials considered.

According to this principle, any mechanical characteristic of the material can be represented in the form of a single function of a reduced parameter X such as:

$$X = \left(\frac{t}{a_T} \right)$$

where a_T is a shifting factor depending on the test temperature T and on the reference temperature T_s .

For the case of bituminous materials, this function takes the form:

$$a_T = \exp 2.5179 \cdot 10^4 \left(\frac{1}{T} - \frac{1}{T_s} \right) \quad (4)$$

with T and T_s expressed in degrees Kelvin.

This change of variables, from t, T to X, makes it possible to plot a master curve from the experimental results obtained at different temperatures. By applying this principle to the viscosity, it may be demonstrated that:

$$\eta(t, T) = a_T \cdot \eta \left(\frac{t}{a_T} \right)$$

This clearly shows that one may construct the viscosity master curve for a reference temperature chosen anywhere in the experimental range, by operating a double shift of the different isothermal curves in a bilog representation. The magnitude of the shifts are equal to $-\log(a_T)$. The master curve obtained by applying this operation to the results given in Figure 6 is displayed in Figure 7.

As a result it is clear that all the materials obeying equation 3 will have a viscosity function in the form:

$$\eta(t, T) = \eta_0 \cdot a_T \cdot \eta \left(\frac{t}{a_T} \right)^b \quad (5)$$

where η_0 is the viscosity measured at $t = 1s$ and $T = T_s$.

Table 1 gives the values of the parameters η_0 and b obtained for different types of poured asphalts and prefabricated sheets.

Seasonal Temperature Variations

Because most types of waterproofing components are temperature susceptible, it proved to be very important to take seasonal temperature variations into consideration when making long-term predictions.

For this purpose, a temperature function of the following form was used:

$$T(t) = T_1 + T_2 \cdot \sin \left(\frac{2\pi(t_0 + t - 106)}{365} \right) \quad (6)$$

in which T_1 is the mean annual temperature; T_2 is the difference between the extreme values of the daily average temperatures observed over one year; t_0 is the starting day; and t is the time expressed in days.

The prediction model now can be applied by introducing formulas 2, 4, 5 and 6 into the main equation 1.

CREEP SLIDING OF DIFFERENT WATERPROOFING SYSTEMS

The prediction method presented above allows different types of waterproofings to be compared from the viewpoint of their tendency to slide by creep under identical loading and temperature conditions.

The standard conditions used to carry out the calculations are:

total thickness of the upper layers: $h_1 + h_2 = 11\text{cm}$,
 specific gravity of the upper layers: $\rho_1 = \rho_2 = 2.7\text{ g/cm}^3$,
 slope of the base: 6 percent,
 temperatures: $T_1 = 22.5\text{C}$, $T_2 = 12.5\text{C}$,
 starting day: July 1,
 total service time: $t_1 = 5\text{ years}$.

Displacements were calculated for 13 different waterproofings having the characteristics displayed in Table 1.

The parameters of the viscosity function were determined on the basis of twelve creep tests per waterproofing type. Each specimen was extracted from a full scale test site where the actual laying conditions were closely reproduced.

It may be stated from the results presented in Figure 8 that:

- Large differences are seen in the resistance to sliding of the different waterproofings. The sliding of product 3 exceeds that of product 5 by a factor of the order of 100.
- Preformed sheets welded to the base slide less than sheets glued with bitumen.
- It is possible to conceive poured asphalts displaying sliding of the same order of magnitude as those caused by welded sheets (Products 15, 13/14).
- Addition of APP (Product 16) does not always contribute to reduce the sliding trend of poured asphalt.
- The binder type is one of the main features determining the risk of sliding of poured asphalts. Product 13/14 is a very hard bitumen, whereas C 54 is very soft.

INFLUENCE OF VIBRATIONS ON POURED ASPHALT WATERPROOFING

Due to the particular laying technique associated with poured asphalt waterproofing, no adhesion exists between these materials and the base. Vibration may thus influence sliding in two ways: by reducing the friction between the concrete base and the waterproofing, and by modifying the viscosity parameters of the waterproofing and increasing the associated creep.

Friction at the Waterproofing Bridgedeck Interface

In order to analyze the influence of vibration on friction at the concrete-waterproofing interface, measurements were made of the sliding thresholds of various test specimens with different types of interfaces under various test conditions. The sliding threshold is the minimum amplitude of constant-frequency vibration which causes the waterproofing to slide. The threshold values found were compared to each other and to the amplitudes of vibration which can be expected in real structures. The following parameters were considered in the study:

- slope of the support: 4 to 10 percent,
- vertical pressure: 1000 to 3000 N/m² which corresponds to a pavement thickness of 4 to 12cm.
- type of interface: non-woven fiber glass sheet or woven fiber glass sheet.
- number of interfaces: 1 or 2,
- texture of the concrete: smooth, medium-rough or rough.

Measurements

A sketch of the measuring equipment is given in Figure 9. The test specimen is placed on an inclinable support and

subjected to a sinusoidal vibration signal of adjustable amplitude and frequency. A displacement sensor connected to a plotter makes it possible to determine the sliding threshold by gradually increasing the amplitude of the vibration signal while keeping the frequency constant.

For each parameter involved in the study, a series of measurements was made at frequencies from 4 to 20Hz. This range corresponds to the frequencies encountered in road bridges.

Results

If there is only one interface, which is the usual practice, only the texture of the support has an influence on the sliding risk. This conclusion results from the fact that a sliding threshold significantly different from the value of the amplitudes corresponding to the gravity (1g) was found only in the case of a perfectly smooth support. In this case the other parameters, slope, pressure and type of interface, have no significant influence on sliding threshold values as shown by the straight line of test no. 24 in Figure 10. The amplitude of vibration that corresponds to these thresholds is well above the amplitudes encountered in bridges during a series of measurements carried out in Belgium.

If there are two interfaces, which is rather unusual, the various parameters considered in the study do have a significant influence on sliding, because the sliding occurs between the two interfaces and not between the interface and the concrete. In this case, sliding thresholds should be reduced by the coefficients given in Table 2.

Test no. 37 in Figure 10 shows that even then the amplitudes of vibration which are necessary to cause sliding are higher than those actually encountered.

Creep of Mastic Asphalt

In order to demonstrate a possible effect of vibration on the creep of mastic asphalt mixes, a comparison was made between the viscosity parameters of identical samples subjected either to a shear test without vibration or to an identical test with vibration.

Measurement

The measuring equipment is the same as for determining sliding thresholds (Figure 9), except that the mastic asphalt is bonded to its support. The component of the ballast's weight acting in the direction of the slope of the support causes the waterproofing to shear. The flow curves, from which the viscosity parameters are derived, are continuously recorded and processed by the computer.

The tests were carried out under the following conditions:

- slope: 10 percent,
- temperature: 45C
- vibration frequency: 5Hz,
- vibration amplitude: 0.5mm.

The characteristics of the vibration signal constitute an unfavorable limit. The amplitude corresponding to the frequency of 5Hz is considerably higher than that encountered in reality (Figure 10). The comparison was made for three pairs of test specimens representing mastic asphalt mixes most frequently used in Belgium.

Results

The viscosity curves obtained after the first shear test, either static or dynamic, on six specimens representing three dif-

ferent materials are shown in Figure 11. Although the shape of the curves is identical for the same materials, it has not been possible to find any systematic action of vibration.

In order to find out whether the dispersion of the curves was due to a possible effect of vibration or to a simple heterogeneity of the samples, a second series of tests was carried out. The waterproofings which were first subjected to a static test now underwent a dynamic test and vice versa.

Figure 12 shows the viscosity curves obtained for one of the materials. In such a representation, one should consider the cumulative duration of the two tests. The beginning of the curve depicting the second test corresponds to the duration of the first test. It appears that the viscosity curves of the second test come into line with the viscosity curves of the corresponding materials as determined during the first test, which are practically taken as asymptotes.

It can therefore be concluded that the dispersion of viscosity curves which has been found arises from the heterogeneity of the materials and that vibration has no influence whatsoever on the creep of these materials.

CONCLUSIONS

Formula 1 makes it possible to predict the sliding of pavements due to creep. The input data are the physical characteristics of the structure as well as the viscosity

parameters of the waterproofing course. The latter are determined by means of a shear test.

A comparison of the tendency of various waterproofings to creep sliding shows that sheets glued with bitumen can slide up to 100 times more than welded sheets, and that it is possible to design mastic asphalt mixes which present little risk of sliding.

Laboratory measurements have shown that vibration has no influence on the risk of sliding, neither through creep phenomena nor through loss of friction between the bridge deck and a nonadherent waterproofing course.

REFERENCES

- ¹ J. Fenijn and R.C. Krooshof, The Sliding-Plate Rheometer. A Simple Instrument for Measuring the Viscoelastic Behaviour of Bitumens and Related Substances in Absolute Units, Proceedings of the Canadian Technical Asphalt Association, Winnipeg, 1970.
- ² C. DeBacker, Influence des vibrations des ponts routiers sur la fatigue de leurs revêtements bitumineux, Symposium "Long-term observation of concrete structures", Budapest, September 17-29, 1984, Organized by Rilem Committee 45-LTO.

ACKNOWLEDGEMENTS

This project is sponsored by the IRSIA (Institut pour l'Encouragement de la Recherche dans l'Industrie et l'Agriculture), which the authors wish to thank for its financial support.

A. Mastic asphalt mixes

No.	Type	Thickness (mm)	Filler %	Binder			Viscosity	
				%	pen (1/10 mm)	T _{R and B} °C	η_0 (Pa.s)	b
11	"German"	12.9	41.5	13.2	41	56	$1.63 \cdot 10^7$	0.50
12	"Modified Belgian"	16.4	47.8	14.7	43	56	$7.77 \cdot 10^6$	0.55
13/14	"Belgian"	17.0	48.9	14.5	20	76	$1.23 \cdot 10^8$	0.48
15	"SBS"	17.4	36.9	13.8**	96**	62**	$2.66 \cdot 10^6$	0.80
16	"APP"	14.4	38.5	14.5**	24**	66**	$2.89 \cdot 10^7$	0.49
54		10.0	30	15.0	54	52	$4.4 \cdot 10^6$	0.43

B. Preformed sheets

No.	Type	Thickness (mm)	Description of the system	Viscosity	
				η_0 (Pa.s)	b
5	Welded sheet	4.4	Bitumen-polypropene reinforced with a non-woven polyester sheet	$5.6 \cdot 10^6$	0.65
8		3.8	Bitumen-elastomer reinforced with a non-woven polyester sheet	$2.0 \cdot 10^7$	0.53
9		4.6	Bitumen-polypropene reinforced with a non-woven polyester sheet + non-woven glass fiber sheet	$9.41 \cdot 10^6$	0.56
3	Sheets glued with bitumen	6.8	Grooved flexible PVC sheet without reinforcement + protective bitumen layer	$4.71 \cdot 10^7$	0.28
6		6.2	Bitumen-elastomer reinforced with a polypropene	$5.17 \cdot 10^6$	0.50
7		3.1	Ethene copolymer strengthened with a non-woven glass fiber sheet	$1.69 \cdot 10^8$	0.30
10		3.8	Coal tar pitch + copolymer, without reinforcement	$7.06 \cdot 10^7$	0.24

* sample taken from a bridge pavement showing severe sliding

** purely indicative values as the traditional methods of analysis are not adapted for the total recovery of polymer-based additives

Table 1 Description of the waterproofing systems

		Non-woven glass fiber sheet		Woven glass fiber sheet	
Slope Load	4 %	10%	4 %	10 %	
	1000 N/m ²	0.84	0.63	0.90	0.54
3000 N/m ²	0.98	0.86	0.95	0.64	

Table 2 Coefficients for reducing the sliding thresholds resulting from the reference test (one interface, smooth support, 10 percent slope, load of 3000 N/m² in the case of two interfaces)

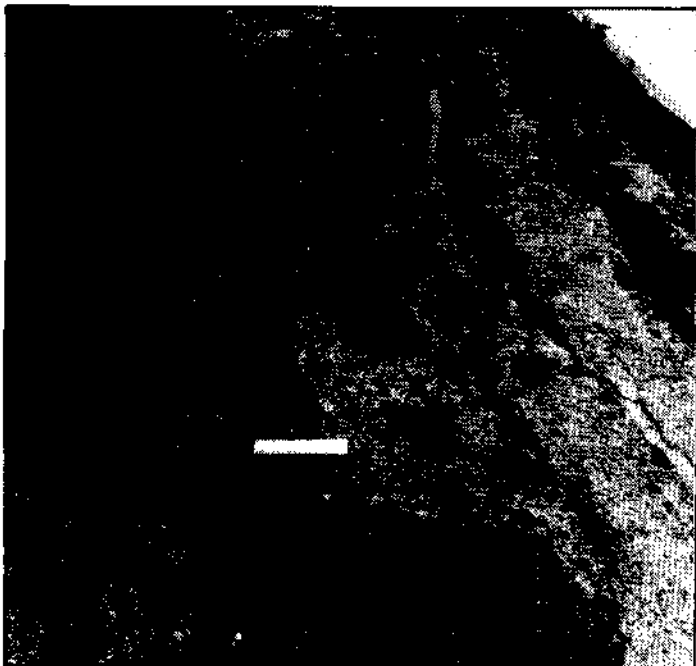


Figure 1 Aspects of cracks in a bridge pavement due to the sliding of the waterproofing system

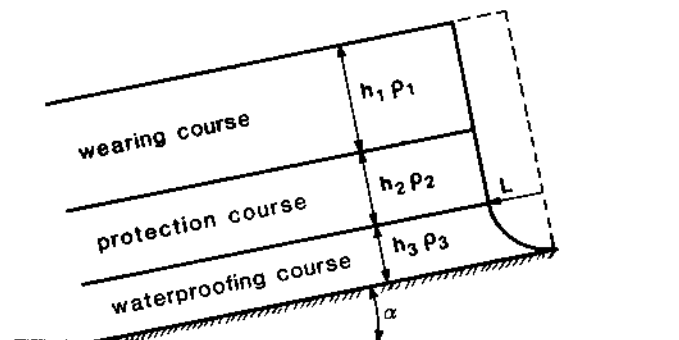


Figure 2 Sketch of a road structure on a bridge

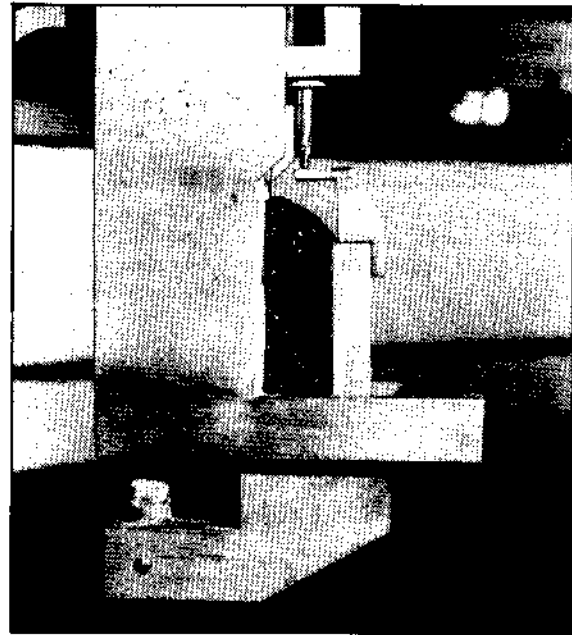


Figure 3 Sliding plate rheometer

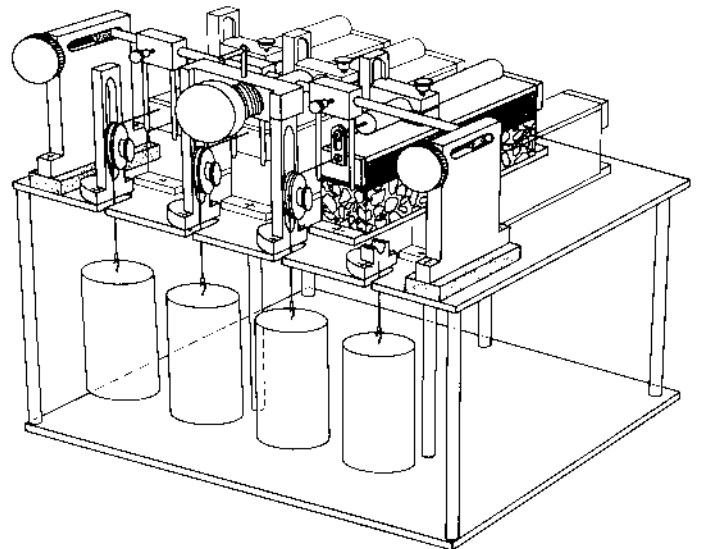


Figure 4 Shear apparatus with four units

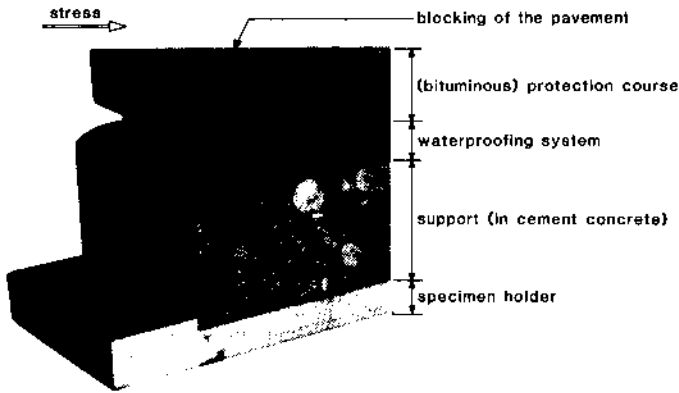


Figure 5 Aspect of the deformation of a test specimen made from a waterproofing system

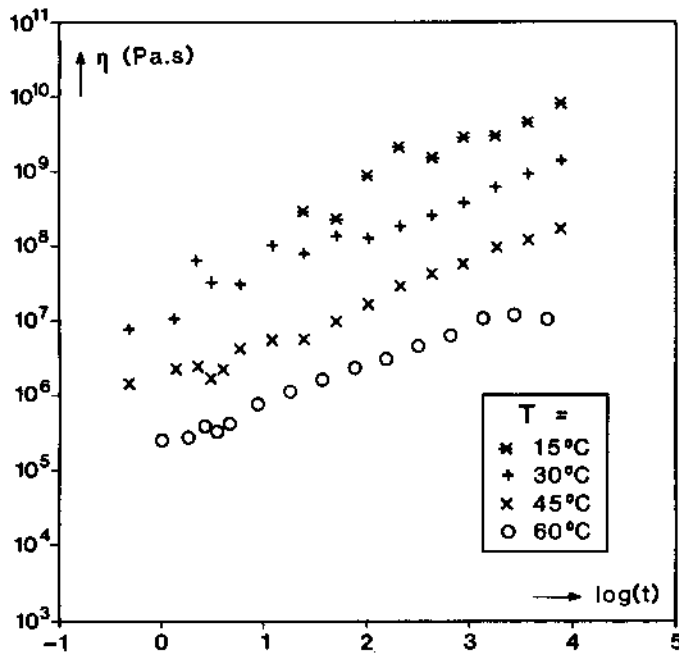


Figure 6 Isotherms of the viscosity of a waterproofing mastic

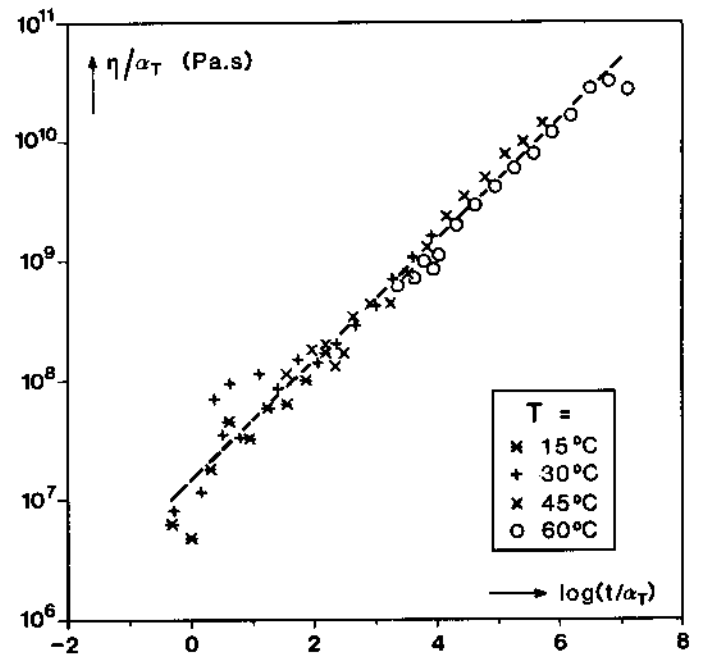


Figure 7 Master curve of apparent viscosity ($T_s = 30^\circ\text{C}$)

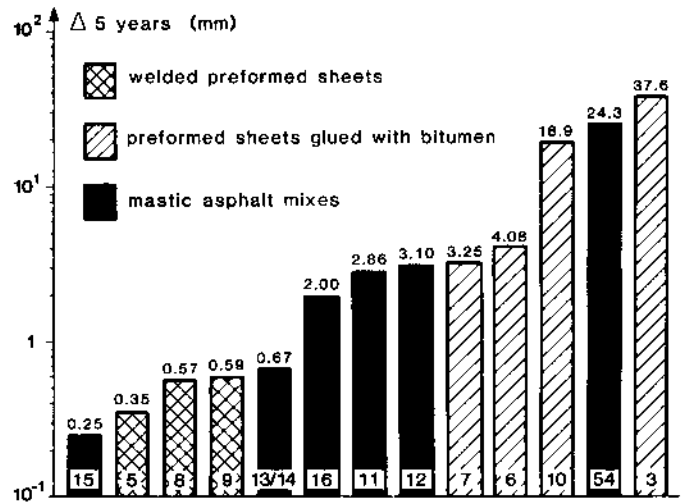


Figure 8 Pavement displacements due to the sliding of water-proofings

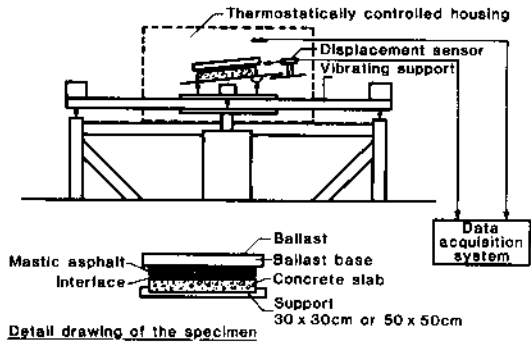


Figure 9 Equipment for measuring pavement sliding due to vibrations

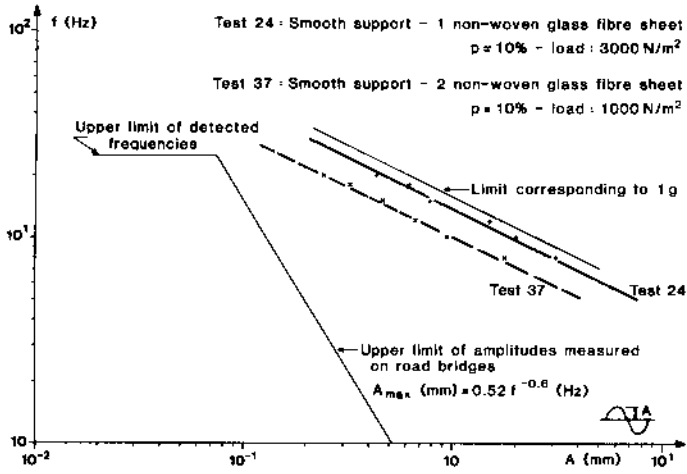


Figure 10 Sliding thresholds

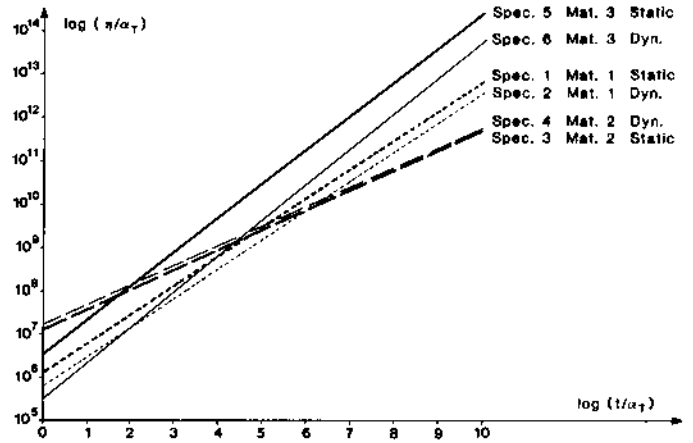


Figure 11 Viscosity curves of waterprooings submitted to a static or dynamic shear test

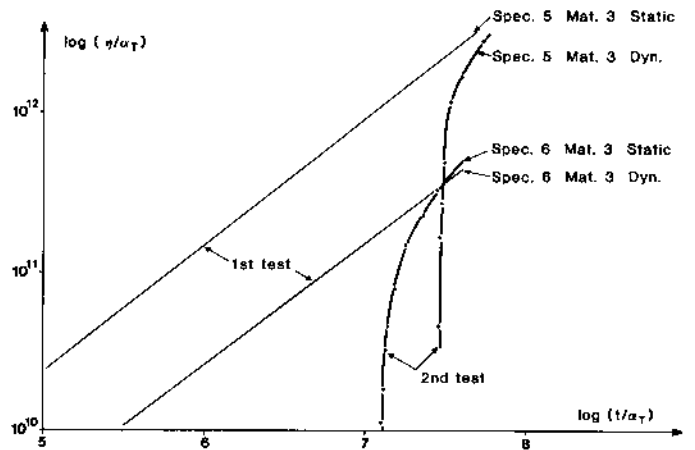


Figure 12 Viscosity curves—Comparison of static and dynamic tests